Simulating flow in porous media

Derek Y. C. Chan and Barry D. Hughes

Department of Mathematics, University of Melbourne, Parkville, Victoria 3052, Australia

Lincoln Paterson

Division of Geomechanics, Commonwealth Scientific and Industrial Research Organization,
P.O. Box 54, Mount Waverley, Victoria 3149, Australia

Christina Sirakoff

Department of Mathematics, University of Melbourne, Parkville, Victoria 3052, Australia

The problem of two-phase fluid flow in statistically homogeneous but random porous media is addressed. Particular emphasis is placed on the role of the stochastic nature of the porous medium in the development of unstable interfaces at large mobility ratios. A formalism is developed in which the random nature of a real porous medium can be incorporated quantitatively into a numerical simulation scheme based on a discretization of the continuum fluid-mechanical equations. In particular, it is not necessary to set the discretization length close to the pore scale and to perform a detailed structural analysis of the microgeometry in order to characterize the random nature of the porous matrix. The formalism is based on the concepts of *tubes* and *chambers* which give rise, on the discretization length scale, to random hydrodynamic conductivity and fluid capacity, respectively, and on larger scales to the macroscopically determined permeability and porosity, respectively. In the absence of detailed information about the statistical properties of the random medium at the discretization length scale, a maximum entropy criterion is used to deduce the most random distribution of properties of tubes and chambers consistent with macroscopically observable quantities. This criterion reveals the fundamental significance of an exponentially distributed fluid capacity. A number of numerical experiments are reported. The relation of the present simulation algorithm to diffusion-limited aggregation (DLA) and related algorithms for the simulation of two-phase flows is revealed, and exponentially distributed fluid capacity is again found to be of fundamental significance. In particular, it is found that a number of further assumptions which are physically plausible but difficult to justify rigorously are required to relate the DLA and similar "random-walk" models to a fluid-mechanical model based on the equations of continuum mechanics applied to a stochastic medium.

I. INTRODUCTION

Porous media encountered in nature vary widely in their structural characteristics. In this paper we address the practical quantitative modeling of flow in microstructured porous media, with particular reference to unstable two-fluid displacements. The treatment is based on the continuum equations of hydrodynamics as applied to a random medium, rather than phenomenological stochastic rules. In principle, one may treat microstructure by making a detailed model which includes the chaotic geometry and topology of the porous medium resolved down to the length scale of an individual pore. While such an approach is valuable in providing insight into the local behavior of flow, it is impracticable for the analysis of flow on the scale of oil reservoirs, aquifers, or packed-bed reaction systems. Our goal is to incorporate the effects of the random nature of the microstructure without having to resolve to the finest length scales.

The structural characteristics of porous media are manifested only very crudely in the classical continuum equations governing flow: the continuity equation for the volume flux (superficial velocity) q,

$$\nabla \cdot \mathbf{q} = 0 \tag{1.1}$$

and Darcy's law relating the volume flux q of a Newtonian fluid to the gradient of the pressure P:

$$\mathbf{q} = -(k/\mu)\nabla P . \tag{1.2}$$

The constants μ and k are, respectively, the shear viscosity of the fluid and the permeability (a property of the porous medium, with the dimensions of the square of a length). For flow of a single fluid within a fully saturated porous medium, the overall modeling of gross features of the flow along these lines requires only the simultaneous solution of Eqs. (1.1) and (1.2), which reduce to Laplace's equation $\nabla^2 P = 0$. For multiphase flows, it is necessary to supply a boundary condition at the interface between two fluids, if the fluids are immiscible, or to prescribe the mixing mechanism for the transition from one pure fluid to another in the miscible case. In the present paper the discussion of multiphase flow is confined to the simultaneous flow of two effectively immiscible fluids through a porous

material. Immiscibility requires the existence of an inter-facial tension, but we shall ignore the dynamical effects of the interfacial tension for the time being. As a result the pressure is continuous across the fluid interface.[1] If the interfacial tension σ is large, the neglect of its dynamical effects requires the assumption of a sufficiently rapid typical flow velocity V. More explicitly, the capillary number

$$Ca = \mu V / \sigma \qquad (1.3)$$

must be large. When the interfacial tension is low, the flow process must be restricted to timescales over which diffusional mixing may be neglected. Equivalently, we must not attempt to resolve the structure of the flow on any finer length scale than the maximum separation between the pure fluids, i.e., the maximum width of the transition zone. For incompressible fluids, the only case treated here, the volume flux normal to the interface must also be continuous. The instantaneous velocity $\mathbf{v}$ of the moving interface in a porous medium should be distinguished carefully from the volume flux $\mathbf{q}$. The relation between them involves the porosity ϕ, the void fraction in a macroscopic sample of the porous medium:

$$\mathbf{v} = \mathbf{q}/\phi \; . \qquad (1.4)$$

The volume flux $\mathbf{q}$ is an underestimate of the interface velocity.

Another consideration in multiphase flows is the different wetting characteristics of the driving and driven fluid on the porous matrix. Such capillarity effects may assist or hinder the displacement process as well as alter the detailed nature of any unstable fluid interfaces. In this paper we shall defer addressing this issue and assume that the wetting properties of different fluids as are negligible compared to the driving pressure gradients.

Conditioned upon the foregoing assumptions, Eqs. (1.1), (1.2), and (1.4), together with the condition of continuity of the pressure field at the interface, appear to give a complete description of two-phase flow in a porous medium. However, when a less viscous fluid displaces a more viscous one, the interface between the fluids may become unstable to small-amplitude disturbances. This instability may be suppressed or enhanced by surface tension or wetting effects and buoyancy effects. It is intrinsically a low-Reynolds number problem entirely contained in the linearized Navier-Stokes equations and its boundary conditions. It has no direct connection with the instabilities associated with the transition to turbulence for high speed flow governed by the nonlinear Navier-Stokes equations. The instability phenomenon has long been known in the petroleum industry as an impediment to the enhanced recovery of oil by water flooding, and is now usually described as *fingering*. The severity of the instability is governed by the mobility ratio, defined as

$$M = \frac{\mu_1}{\mu_2} \qquad (1.5)$$

where μ_1 is the viscosity of driven fluid and μ_2 the viscosity of driving fluid. The greatest fingering occurs at infinite mobility ratio, i.e., an inviscid fluid displacing a Newtonian fluid.

In two dimensions, the differential equations governing flow in a porous medium coincide with those governing flow in a Hele-Shaw cell,[2] i.e., flow between two closely-spaced parallel plates. The boundary conditions at the interface between two fluids in a Hele-Shaw cell may be written down for arbitrary capillary number, and reduce to the boundary conditions stated above for the porous medium in the limit that the capillary number becomes infinite. For finite capillary numbers, the Hele-Shaw cell boundary conditions are inappropriate for porous media. The hydrodynamic instability which arises when a less viscous fluid displaces a more viscous one in a Hele-Shaw cell was first studied by Saffman and Taylor[3] and is usually called the Saffman-Taylor instability.

The ability of the continuum equations to predict fingering for both porous media and Hele-Shaw cells is gratifying. However, since these equations contain only two medium-dependent properties, the permeability k and the porosity ϕ, they predict that for a given pair of Newtonian fluids (i) all porous media with the same values of k and ϕ should yield statistically identical fingering patterns, and (ii) two-dimensional unstable displacements in porous media should yield patterns indistinguishable from those which may be generated in Hele-Shaw cells with the appropriate plate spacing (at least at large capillary number, so that the effects of surface tension in the Hele-Shaw cell, which do not represent the effects of surface tension in a real porous medium, are suppressed). This prediction is contradicted by experiments.[4]

The reasons for the discrepancy are now understood. In the classical modeling of flow in porous media, the medium is regarded as a *structureless* continuum completely characterized by a porosity and a permeability. Real porous media usually have a chaotic microstructure to which the classical continuum treatment pays no attention. The neglect of microstructure restricts the applicability of the continuum equations and indeed the notions of permeability and porosity to sufficiently large length scales. In quantifying the concepts of a porosity and a permeability to be used in a continuum description of fluid flow in porous media, Bear[5] and Bear and Bachmat[6] discuss the concept of the representative elementary volume (REV). A REV is defined so that it contains solid phase and void space no matter where it is placed in the porous medium under consideration. The length scale defining the REV must be taken to be large enough so that the microstructure cannot be resolved, but must be small enough so that systematic variations in properties (associated in a geological context, for example, with stratification) are also not encountered. For the problem of two-fluid displacement in porous media, it has been found that fluctuations in the material properties are central to the development of instabilities in the form of fluid fingering.[7] Not all naturally occurring porous media contain the same degree of microscopic randomness, so that it is as inappropriate to work with a single model of the randomness as it is to ignore the randomness completely. It is only for the least random porous media (if at all) that the Hele-Shaw cell analogy may be relevant to fingering in porous media.

As a consequence of the preceding considerations, it is clear that a particularly severe test of any simulation scheme for two-phase flow in porous media is the quantitative prediction of the interface motion for unstable displacements. A continuum limit of the Witten and Sander[8] diffusion-limited aggregation (DLA) algorithm is identical to the equations governing flow in a Hele-Shaw cell or a structureless classical porous medium, so that one might expect a similarity in shape between DLA clusters and fingers in a Hele-Shaw cell. Paterson[9] noticed that this is not the case. Rather there is a striking similarity between the shape of diffusion-limited aggregation clusters and the shape of fingers observed in *random* porous media. This again demonstrates the importance of a correct treatment of microstructure in a porous material. To characterize two-fluid fingering completely, we need to arrive at an understanding of the role of porous medium structure and of the role of the fluid combination (wetting or miscibility properties). In this paper we do not examine fluid properties. We concentrate only on the properties of the medium. This enables us to emphasize the difference between Hele-Shaw cell fingering and porous media fingering. As a consequence of our analysis, we are able to make some precise statements concerning the physical basis and range of validity of DLA as a simulation scheme for Hele-Shaw cell and porous media fingering.

Some preliminary investigations of these issues have been made in earlier papers of the authors.[7,10] In particular, we introduced the concept of fluid capacity at a specified length scale of a porous medium[7,10] which allows us to characterize quantitatively the degree and nature of the structural randomness of a porous material at any operationally convenient length scale. In this paper, we show how this concept can be incorporated in numerical simulations based on the continuum equations of fluid flow in porous materials. This represents a consistent way of marrying together the structural randomness of a porous material with deterministic equations of hydrodynamics and provides a physically based alternative to phenomenological stochastic simulation schemes. We shall be concerned here only with statistically homogeneous porous materials, so that there are no systematic variations on large length scales; all variations are associated with microstructure, and amenable to statistical description.

As a corollary to our analysis, we are able to provide a quantitative explanation for the observed applicability of the diffusion-limited aggregation model to simulation of unstable flows in some real disordered porous media. The applicability rests on (i) the microstructure of the material at the simulation discretization length scale being close to an exponential fluid capacity distribution; and (ii) the discretization length scale coinciding with a natural length scale in the porous material set by the wetting or miscibility properties of the fluids.

II. MODELING A POROUS MEDIUM

In the continuum description which ignores the details of microstructure, the properties of a porous medium are modeled solely in terms of two constants, the permeability k and the porosity ϕ. These two constants arise respectively from the resistance the porous medium offers to the flow and from the ability of the porous medium to store fluid. Ultimately, both properties come from microstructure and are interrelated, but there is no universal relation between them. In nature, k and ϕ can vary over many orders of magnitude for different types of porous material, but for a given macroscopically homogeneous sample, k and ϕ are constant. Within a given material, the flow resistance and the ability to store fluid (or which the permeability and porosity are macroscopic manifestations) fluctuate over small length scales. We contend that so far as fingering is concerned, the inhomogeneity in flow resistance may be less significant than the inhomogeneity in the ability to store fluid. We begin by advancing arguments in support of this claim and subsequently turn to the question of the definition of the ability of a material to store fluid, introducing the notion of "fluid capacity," which is not synonymous with porosity.

A. Illustrative examples

Consider first the oversimplified but illustrative problem of a one-dimensional displacement in a composite classical porous medium which consists of a large number N of slabs of equal thickness L/N, but differing permeabilities k_i. The volume flux q is the same in each slab, and if we denote the pressure drop across the ith slab by P_i, we have from Darcy's law that $q = k_i P_i N/(\mu L)$. The total pressure drop is

$$P = \sum_i P_i = (\mu L q /N) \sum_i k_i^{-1} , \tag{2.1}$$

and we obtain an equivalent Darcy's law for the composite system:

$$q = k_{\text{eff}} P /(\mu L) \quad \text{where} \quad k_{\text{eff}}^{-1} = (1/N) \sum_i k_i^{-1} , \tag{2.2}$$

so that the effective permeability k_{eff} and the slab permeabilities k_i are related like the total resistance of a set of resistors in parallel. The law of large numbers[11] guarantees that if the slab permeabilities k_i are independently and identically distributed random variables, then k_{eff}^{-1} converges with probability 1 to $\langle k^{-1} \rangle$, the average of the inverse permeability of a slab. The effect of any one slab, whether very permeable or scarcely permeable, is hardly felt in the overall resistance to flow; only the spatial average of the permeabilities matters. While this strong spatial-averaging effect is not so easily demonstrated in two- or three-dimensional composite porous media, it still occurs, and the value of the effective permeability of a sample can be estimated provided the sample size is sufficiently large compared with the length scale associated with permeability fluctuations.[12]

While the hydrodynamic drag on a macroscopic quantity of fluid is strongly influenced by the large-scale properties of the porous medium, the instantaneous velocity of the interface between two fluids senses the small-scale structure of the porous medium. This comes from the inequivalence of the interface velocity and the volume

flux [Eq. (1.4)], and is most easily demonstrated in the case of an inviscid fluid displacing a viscous one. Consider two points on the interface at which the pressure gradients in the displaced viscous fluid are equal. If the porosity fluctuates, then of the two positions on the interface, that entering the region of lower porosity travels faster.

We illustrate here the distinction between the effects of hydrodynamic resistance, which are averaged over space, and the purely local effects of fluctuations in the ability to store fluid in the vicinity of the advancing interface, with a simple one-dimensional problem in which a Newtonian fluid of finite viscosity is displaced by an inviscid fluid. The viscous fluid is withdrawn from the origin and the interfaces between the fluids are located at points $x=-l(t)<0$ and $x=r(t)>0$. (See Fig. 1.) A constant pressure drop P_0 is maintained between each fluid interface and the origin. Since the pressure satisfies Laplace's equation, the pressure gradients on the left and right of the origin have magnitudes P_0/l and P_0/r, respectively. The magnitudes of the volume fluxes v_l and v_r on the left and right of the origin are given by Darcy's law (1.2), so that

$$v_l=(k/\mu)(P_0/l) , \quad v_r=(k/\mu)(P_0/r) , \tag{2.3}$$

where k is the permeability and μ is the viscosity of the displaced fluid. The instantaneous velocities of the interfaces are given by

$$dl/dt=-v_l/\phi , \quad dr/dt=-v_r/\phi , \tag{2.4}$$

where ϕ is the porosity. In an *ideal* porous medium where there are no fluctuations in material properties, k and ϕ are constants and the motion of the interfaces can be found by solving Eqs. (2.3) and (2.4) for $l(t)$ and $r(t)$. One finds that

$$l^2(t)-l^2(0)=r^2(t)-r^2(0)=-\frac{2kP_0}{\mu\phi}t . \tag{2.5}$$

In a statistically homogeneous rather than ideal porous medium the interface will not move in this deterministic manner, as there is a stochastic element in the displacement process. One way to build in randomness is to make the permeability k and porosity ϕ erratic functions of position, $k(x)$ and $\phi(x)$, respectively. Equations (1.1) and (1.2) now become

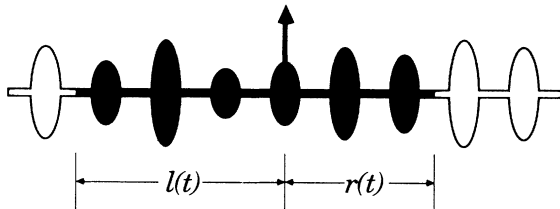$$\frac{\partial q}{\partial x}=0 \text{ and } q(x,t)=-\frac{k(x)}{\mu}\frac{\partial P}{\partial x} . \tag{2.6}$$

FIG. 1. A one-dimensional displacement process.

These equations hold on the intervals $-l(t)<x<0$ and $0<x<r(t)$. Applying the boundary conditions $P=0$ at $x=0$, $P=P_0$ at $x=r(t)$, and $P=P_0$ at $x=-l(t)$, and noting that $q(r(t),t)=\phi(r(t))dr/dt$ and $q(-l(t),t)=-\phi(-l(t))dl/dt$, we readily show that

$$\frac{dl}{dt}=-\frac{P_0}{\mu\phi(-l)}\left[\int_{-l}^0\frac{d\xi}{k(\xi)}\right]^{-1}$$

and   (2.7)

$$\frac{dr}{dt}=-\frac{P_0}{\mu\phi(r)}\left[\int_0^r\frac{d\xi}{k(\xi)}\right]^{-1} .$$

It is now quite explicit that in this simple problem the instantaneous velocities of the interfaces are determined by the instantaneous porosities and globally averaged permeabilities. If the permeability is a random function of position, with suitable stochastic translational invariance and correlation length δ for permeability fluctuations, so long as $l\gg\delta$ and $r\gg\delta$ we will have

$$\frac{1}{l}\int_{-l}^0\frac{d\xi}{k(\xi)}\approx\frac{1}{r}\int_0^r\frac{d\xi}{k(\xi)}\approx\left\langle\frac{1}{k}\right\rangle\equiv\frac{1}{k_{\text{eff}}} . \tag{2.8}$$

The differential equations governing the motion of the interfaces become

$$\frac{dl}{dt}=-\frac{P_0k_{\text{eff}}}{\mu l\phi(-l)} \text{ and } \frac{dr}{dt}=-\frac{P_0k_{\text{eff}}}{\mu r\phi(r)} , \tag{2.9}$$

and so even if we begin with the left and right interfaces equidistant from the origin, the relative speeds of the interfaces may be very different. Consider two displacement processes in different one-dimensional random media. When are these two displacement processes statistically equivalent? So far as the permeability is concerned, it suffices that the two media have the same effective permeability k_{eff}. However, it is essential that the two media have not merely the same average porosity, but the exact same porosity distribution.

Our illustrative examples are one dimensional, but in two- and three-dimensional systems, the same general conclusion holds. The total resistive force on a large region of fluid is derived from the sum of the resistive forces over many small parcels of fluid, and will reflect the average properties of the porous material. However, the motion of the interface between fluids remains highly sensitive to small-scale fluctuations in the ability to store fluid.

B. The notion of fluid capacity

In the preceding examples, we considered idealized porous continua with variable porosities and permeabilities. One cannot really take the notions of permeability and porosity down to arbitrarily small length scales, since they are essentially macroscopic or "Darcy scale" concepts forced on us by the modeling of the porous material as a continuum. The notion of a variable porosity is physically sensible only if the length scale on which the porosity is asserted to change far exceeds the typical size of the individual pores. We can, however, replace the porosity with a new quantity which may be defined and

measured on any preassigned length scale. We define[7,10] the fluid capacity, a dimensionless quantity, to be the void space per specified length λ in one dimension, the void space per specified area λ^2 in two dimensions, and the void space per specified volume λ^3 in three dimensions. In principle, our characteristic or resolution length scale λ can be assigned any desired value. In practice, as discussed below, it is the grid or mesh size in a standard discretization of the continuum equations of fluid mechanics. We shall denote the fluid capacity of a porous medium by ϕ; it is a random variable, not a determinate number. Its statistical distribution may be measured.[10] For the usual porosity we introduce the symbol $\langle \phi \rangle$; the $\langle \ \rangle$ serves to remind us that porosity is a macroscopic or Darcy scale quantity, and a determinate number. If λ is on the Darcy scale, i.e., in the limit $\lambda \to \infty$, the fluid capacity ϕ becomes identical to the porosity $\langle \phi \rangle$. In other words, in the limit $\lambda \to \infty$, ϕ converges to $\langle \phi \rangle$ in an appropriate probabilistic sense. In three dimensions, fluid capacity, like porosity, is constrained to be less than unity; no such constraint exists in one or two dimensions. If λ is on the pore scale, the fluctuations in the fluid capacity correspond to the pore size distribution.

It is possible to define as a companion for the fluid capacity an analogous flow resistance random variable which converges to the usual permeability as $\lambda \to \infty$. In view of the examples discussed above, which indicate that the effective resistance to flow only appears in some averaged sense and hence only has secondary influence upon the fingering phenomenon, the need for such a concept is perhaps less pressing than the need for the concept of fluid capacity, and we do not pursue it. We shall, however, take the precaution of inserting $\langle \ \rangle$ to remind us that permeability $\langle k \rangle$, like porosity $\langle \phi \rangle$, is a Darcy scale concept.

C. An algorithm for numerical simulations

For our numerical modeling of porous media, we use a simple discretization scheme on the continuum equations of fluid flow. However, we introduce two fundamental elements: tubes and chambers. The tubes are assumed to be of small diameter, and so give rise to a hydrodynamic drag or resistance to flow, but hold a negligible volume of fluid. These tubes connect the grid or mesh points a distance λ apart at which the chambers are located. The chambers are assumed to have volumes much greater than those of the tubes, thus making a negligible contribution to the hydrodynamic resistance of the porous medium, but holding virtually all of the fluid. At macroscopic scales, the tubes give rise to the permeability $\langle k \rangle$ and the chambers to the porosity $\langle \phi \rangle$. Here, as remarked above, the $\langle \ \rangle$ are inserted to emphasize that permeability and porosity are macroscopic observables obtained by averaging over the microstructure. If λ is taken to be on the pore scale, then the tubes may be tentatively identified with pore throats and the chambers with pore bodies, but it is not necessary to take λ on the pore scale, and indeed such an identification of λ would not be practical for reservoir-scale simulations nor might

it always be appropriate on physical grounds, as discussed below.

The joint statistical distribution of chamber volumes and tube resistances is dependent on the length scale λ one chooses. As a general rule, the perceived degree of randomness of the medium is reduced as λ increases, as discussed below. It is conceivable that for some porous media, a distribution with simple scaling properties might suffice for several decades of λ values; such a porous medium would have "fractal" properties. It is more likely, though, that the shape of the distribution will change with λ, since porous media often exhibit statistical heterogeneities with different physical origins on different length scales. The modeling approach we propose is neither intended nor able to resolve any details of the flow on length scales smaller than λ. The range of possible values of λ for simulating a given porous material is clearly limited by physical considerations. At very small length scales, the location of the interface may become ill-defined due to diffusional mixing of the fluids, or to the presence of a capillary fringe zone. The assumption of independence of the fluid capacities of different chambers also limits λ to lengths exceeding the correlation length of the microstructure. These and other considerations restrict us from making λ too small. At the other extreme, aquifers and oil reservoirs often exhibit a systematic stratification, so that λ must be kept somewhat smaller than the length scales associated with stratification, and it may be necessary to subdivide the porous material into a number of regions, each with its own characteristic value of λ.

For simulations using the tubes and chambers approach, the chambers are placed on the sites of a linear chain (for a one-dimensional simulation), a plane square lattice (for a two-dimensional simulation), or a simple cubic lattice (for a three-dimensional simulation). Our numerical simulations reported in Sec. III are confined to one and two dimensions, but the approach is equally applicable to three-dimensional problems. The tubes form the bonds of the lattice. Each bond has length λ which corresponds to a lattice spacing in a finite difference approximation. It is the incorporation of chambers each having a random volume at the lattice sites which distinguishes the present approach from the usual numerical simulation of Darcy's law, and from other models based on networks of random tubes. We shall denote the dimensionless volume of a chamber by ϕ. Physically, ϕ corresponds to the fluid capacity introduced above. The length scale λ used to define the fluid capacity is precisely that to be used for the lattice spacing in the simulation. The optimal choice of λ is the natural length scale associated with the wetting and miscibility properties of the fluids. The prediction of this value of λ is a separate issue, not addressed here.

D. Entropy considerations in fluid capacity distribution

Let us defer for the moment the discussion of the assignment of hydrodynamic resistance to the tubes, and address the problem of selection of the probability density function $f(\phi)$ to be assigned to the dimensionless

chamber volumes or fluid capacity. Intuitively, one expects the effects of microstructure to be greatest when the fluid capacity is distributed as randomly as possible. A measure of the randomness of the probability density function $f(\phi)$ is the (Shannon) entropy[13,14]

$$S\{f\} = -\int_{\phi_{\min}}^{\phi_{\max}} f(\phi)\ln[f(\phi)]d\phi \ , \tag{2.10}$$

where $(\phi_{\min},\phi_{\max})$ is the interval of allowed values of the fluid capacity ϕ, so that our criterion for the most random density $f(\phi)$ supported by the interval $(\phi_{\min},\phi_{\max})$ is that $f(\phi)$ maximize the functional (2.10). The maximum must be sought not over the class of all differentiable functions, but only over those functions which are nonnegative and satisfy the normalization condition

$$\int_{\phi_{\min}}^{\phi_{\max}} f(\phi)d\phi = 1 \ . \tag{2.11}$$

Introducing a Lagrange multiplier α in the usual fashion, we extremize the quantity

$$S^*\{f\} = -\int_{\phi_{\min}}^{\phi_{\max}} f(\phi)\ln[f(\phi)]d\phi + \alpha\int_{\phi_{\min}}^{\phi_{\max}} f(\phi)d\phi \ . \tag{2.12}$$

A sufficient condition for the functional

$$S^*\{f\} = \int_{\phi_{\min}}^{\phi_{\max}} F(f(\phi),\phi)d\phi \tag{2.13}$$

to be (locally) maximized by the function f is that

$$\frac{\partial F}{\partial f} = 0 \quad\text{and}\quad \frac{\partial^2 F}{\partial f^2} < 0 \ . \tag{2.14}$$

With $F(f,\phi) = -f\ln f + \alpha f$ we find that

$$\frac{\partial F}{\partial f} = \alpha - 1 - \ln f \quad\text{and}\quad \frac{\partial^2 F}{\partial f^2} = -\frac{1}{f} \ . \tag{2.15}$$

Thus, imposing only the normalization constraint (2.11), we see that a maximum in the entropy is attained when $f(\phi)$ is the uniform density

$$f(\phi) = \frac{1}{\phi_{\max} - \phi_{\min}} \ , \quad \phi_{\min} < \phi < \phi_{\max} \ . \tag{2.16}$$

The Lagrange multiplier α is determined by the normalization condition (2.11). The entropy for the uniform density (2.16) is

$$S\{\text{uniform density on } (\phi_{\min},\phi_{\max})\} = \ln(\phi_{\max} - \phi_{\min}) \ . \tag{2.17}$$

In the preceding discussion we have inserted only one piece of physical information about the fluid capacity ϕ, viz., an interval $(\phi_{\min},\phi_{\max})$ of allowed values. For a sample of porous material we may at least measure the porosity $\langle\phi\rangle$, so that it is appropriate to restrict the class of functions in which the entropy-maximizing density is sought, by imposing the constraint that the mean of the fluid capacity coincide with the porosity:

$$\int_{\phi_{\min}}^{\phi_{\max}} \phi f(\phi)d\phi = \langle\phi\rangle \ . \tag{2.18}$$

We now maximize the functional

$$S^*\{f\} = -\int_{\phi_{\min}}^{\phi_{\max}} f(\phi)\ln[f(\phi)]d\phi + \alpha\int_{\phi_{\min}}^{\phi_{\max}} f(\phi)d\phi$$
$$+ \beta\int_{\phi_{\min}}^{\phi_{\max}} \phi f(\phi)d\phi \ , \tag{2.19}$$

where α and β are Lagrange multipliers, so that in Eq. (2.13) the integrand becomes

$$F(f,\phi) = -f\ln f + \alpha f + \beta\phi f \tag{2.20}$$

and

$$\frac{\partial F}{\partial f} = \alpha - 1 - \ln f + \beta\phi \quad\text{and}\quad \frac{\partial^2 F}{\partial f^2} = -\frac{1}{f} \ . \tag{2.21}$$

For a prescribed mean fluid capacity $\langle\phi\rangle$ and interval of allowed fluid capacities $(\phi_{\min},\phi_{\max})$, we deduce that the entropy is maximized when the fluid capacity has the probability density function

$$f(\phi) = A\exp(\beta\phi) \ , \quad \phi_{\min} < \phi < \phi_{\max} \ , \tag{2.22}$$

where the constants A and β are determined from the normalization constraint (2.11), and the prescription (2.18) of the mean fluid capacity. In the special case in which the fluid capacity ϕ is permitted to take any positive value (i.e., $\phi_{\min}=0$, $\phi_{\max}=\infty$), we find for the entropy-maximizing probability density the exponential law

$$f(\phi) = (1/\langle\phi\rangle)\exp(-\phi/\langle\phi\rangle) \ . \tag{2.23}$$

The entropy of this density is

$$S\{\text{exponential density on } (0,\infty)\} = 1 + \ln(\langle\phi\rangle) \ . \tag{2.24}$$

Additional constraints may be imposed on $f(\phi)$ if further experimental data is available, so that at any level of knowledge of the properties of the fluid capacity distribution it is possible to find a "most random" medium consistent with the data at hand. Typical data would involve higher moments of the fluid capacity. For example, if the variance of ϕ is known in addition to the mean, one finds a truncated Gaussian density for the most random $f(\phi)$. In the simulations discussed in Sec. III, we afford the exponential density (2.23) special emphasis, not only in view of its appearance as the most random distribution if only the mean fluid capacity is known, but also because of of connections between the tubes and chambers approach and other stochastic simulation schemes discussed in Sec. IV—which is most evident for the exponential fluid capacity distribution.

Fluid capacity distributions are experimentally measurable. Their form depends both on the material being studied and on the length scale λ chosen. The distribution of fluid capacity becomes narrower as λ is increased. The authors have illustrated these points recently,[10] obtaining fluid capacity distributions of random two-dimensional structures corresponding to micrographs of cross sections of real porous materials. For some of the structures studied, a length scale can be found on which the fluid capacity is exponentially distributed; for other materials no length scale gives a good fit to an exponential distribution. When λ is increased, an exponential distribution of fluid capacity is replaced by a Γ distribution.

This is easily proved[10] and is seen in experiments.[10] Increasing the value of λ corresponds to a grouping of chambers to form a composite chamber, similar to the notion of the tunable noise in simulation algorithms.[15,16]

E. Hydrodynamic conductivities

We have not yet addressed the assignment of hydrodynamic conductivities to the tubes. In suitably scaled variables, each tube can be associated with a random hydrodynamic conductivity k, with units the square of a length and mean value the macroscopic permeability $\langle k \rangle$. It is straightforward to generalize the preceding maximum entropy argument to find the most random joint density for the fluid capacity ϕ of a chamber and the conductivities k_i of the tubes which are connected to it. If we prescribe only the mean values of k_i and ϕ, we find that for the most random case, the random variables k_i and ϕ are independent, and exponentially distributed. The independence holds for a wide variety of constraints and is only destroyed if we impose experiment-based constraints linking k_i and ϕ.

While for the purposes of realistic modeling of random porous media one should allow both the chamber volumes and the tube resistances to be random, we shall consider here only the simpler case in which the tubes all have identical hydrodynamic resistance, and the chamber volumes are independently and identically distributed. It is this case which is most easily connected to diffusion-limited aggregation and related algorithms—see Sec. IV. Moreover, as we have noted above, the effects of variability in hydrodynamic conductivity above the pore scale may be smaller than the effects of variable fluid capacity. Also, again as noted above, for the "most random" media, the variations in fluid capacity and hydrodynamic conductivity are independent.

III. NUMERICAL SIMULATIONS

In an earlier paper[10] we have demonstrated how the fluid capacity distributions of some natural and artificial porous materials can be readily measured and thereby provide a direct description of the stochastic properties of random media in terms of our tubes and chambers model. In this section we present some sample calculations of fluid displacement studies in random media. These will serve as illustrations of how our tubes and chambers model of characterizing the stochastic properties of porous media may be combined with the macroscopic equations of fluid flow. We report simulations in one and two dimensions for the displacement of one Newtonian fluid by another. The fluids are treated as immiscible.

A. One-dimensional simulations

In our one-dimensional simulations, we have a withdrawal point at the center site of a finite linear chain. On either side of the center site are placed the same number of chambers. Chamber volumes are independently and identically distributed random variables. Here we have

considered only exponentially distributed chamber volumes. (Some simulations for other distributions of chamber volumes have been reported elsewhere.[7]) Initially all chambers are filled with the driven fluid, and no driving fluid is present. Driving fluid is now introduced at each end of the chain, and driven fluid is consequently forced out through the withdrawal point. The pressure drop between the ends of the chain and the withdrawal point is specified and held constant.

One-dimensional simulations have carried out for a range of mobility ratios [Eq. (1.5)]. This enables us to study the interplay between the size of the system and the mobility ratio. The results are shown in Table I. For the range of system sizes considered here, ratios exceeding 1000 may clearly be taken as infinite, while those smaller than $\frac{1}{1000}$ may be taken as zero.

We consider now, for the case of an infinite mobility ratio, the effects of a change in the value of the length scale λ. Increasing the value of λ corresponds to grouping chambers together and treating them as composite chambers. These composite chambers do not have exponentially distributed volumes, but rather gamma distributions.[10] We commence with the random assignment of exponentially distributed volumes to N chambers on each side of the withdrawal point. This defines a realization of the random medium. We select the length scale λ (≥ 1) by grouping together λ adjacent chambers to form a single composite chamber. The results from averaging over 20 realizations of the model system with different values of λ are shown in Table II. It will be observed that the recovery efficiency is substantially unaltered by a change of an order of magnitude in the value of the length scale λ, at least until the groups of chambers become so large that there are only a couple of chambers on each side of the withdrawal point.

B. Two-dimensional simulations

For our two-dimensional studies, we confine ourselves to the problem of displacing a Newtonian fluid by an inviscid fluid—this is the classic problem of displacement at infinite mobility ratio. According to stability analysis of the continuum Darcy equations, the displacement front in this problem is maximally unstable.[17] The application of our method to Newtonian displacements with finite mobility ratios as well as displacements involving non-Newtonian fluids will be considered elsewhere.

The displacement geometry will be that of a "quarter-five-spot" configuration in which a random porous material, initially saturated with the Newtonian fluid, is confined with a square boundary. The inviscid driving fluid is injected at one corner of the square and the displaced fluid is withdrawn at the opposite corner. Impermeable boundary conditions are imposed on all four sides of the square. The displacement problem is treated in the usual quasistatic approximation in which the pressure distribution P in the Newtonian fluid is governed by the solution of the Laplace equation $\nabla^2 P = 0$ with the following boundary conditions. At the impermeable boundaries, the normal derivative of the pressure $\partial P / \partial n$ vanishes. We can without loss of generality assume $P = 0$ at

TABLE I. Displacement inefficiencies (%) for one-dimensional displacements simulated by a tubes-and-chambers model with exponentially distributed chamber volumes. The mobility ratio M is defined by the viscosity ratio of driven fluid divided by the viscosity of driving fluid. The displacement inefficiency is the percentage of the initial volume of fluid remaining on one side of the withdrawal point when the driving fluid breaks through on the other side. The reported inefficiencies are averages over 20 realizations of a system of given size and mobility ratio.

| M | Number of chambers on each side of the withdrawal point |
	10	100	1000	10 000	32 000
10^{-7}	20.75	6.084	2.261	0.7558	0.3728
10^{-6}	20.75	6.084	2.261	0.7558	0.3729
10^{-5}	20.75	6.084	2.261	0.7557	0.3729
10^{-4}	20.75	6.084	2.261	0.7559	0.3728
10^{-3}	20.76	6.086	2.261	0.7561	0.3729
10^{-2}	20.78	6.112	2.267	0.7593	0.3747
10^{-1}	21.04	6.447	2.336	0.7911	0.3920
1	29.09	10.54	3.593	1.309	0.6871
10^{1}	41.49	25.03	12.81	5.935	3.471
10^{2}	44.42	30.10	18.55	10.53	7.363
10^{3}	44.72	30.80	19.33	11.30	8.127
10^{4}	44.75	30.87	19.41	11.38	8.210
10^{5}	44.75	30.88	19.42	11.39	8.219
10^{6}	44.75	30.88	19.42	11.39	8.220
10^{7}	44.75	30.88	19.42	11.39	8.220
10^{8}	44.75	30.88	19.42	11.39	8.220

the withdrawal corner and $P = 1$ everywhere within the inviscid fluid and at the fluid interface.

We solve the boundary value problem by a finite difference algorithm based on the method of successive over-relaxation.[18] A grid of $N \times N$ nodes, numbered $n = 1, 2, \ldots, N^2$, is placed on the square domain. The grid is taken to have unit spacing, which corresponds to

TABLE II. Variations of the displacement inefficiency with changes in the length scale λ at a mobility ratio of 10^7. The tabulated displacement inefficiency is the percentage of the initial volume of fluid remaining on one side of the withdrawal point when the driving fluid breaks through on the other side. The reported inefficiencies are averages over 20 realizations shown with ±1 standard deviation. There are 8192 chambers (with exponentially distributed volumes) on each side of the withdrawal point.

Length scale λ (numbers of chambers grouped together)	Displacement inefficiency (%)
1	14.28±4.28
2	14.28±4.28
4	14.28±4.28
8	14.25±4.27
16	14.20±4.28
32	14.12±4.27
64	13.94±4.28
128	13.60±4.28
256	12.91±4.29
512	11.60±4.26
1024	9.01±4.50
2048	5.16±2.98

measuring all lengths in units of the resolution length scale λ. These nodes are assumed to be connected by tubes of equal resistance to flow. The tubes are assumed to have negligible volume. The stochastic nature of the porous material is modeled in terms of its ability to store fluid. With each node, we associate a fluid chamber of a particular volume or fluid capacity. The values of the fluid capacities ϕ_n are assigned to each of these chambers according to some statistical distribution. The exponential distribution of fluid capacities is used for most of the calculations given here. This is because, as discussed in Sec. II, when the mean porosity of the porous sample is specified, the exponential distribution corresponds to the most random distribution of fluid capacities. Also, as we shall see in Sec. IV there is a special relationship between the exponential distribution of fluid capacities and the method of simulating flow in porous media based on the diffusion-limited aggregation algorithm.

The fluid displacement process is envisaged as the driving fluid replacing the content of the chambers which were originally occupied by the displaced fluid. At any time during the displacement process, there will be a set of chambers which either have the potential to be filled with the driving fluid or are already partially filled with the driving fluid and partially filled with the displaced fluid. We call these the boundary chambers as they define the fluid interfacial boundary [see Fig. 2(a)]. However, in our discretization scheme to determine the pressure at each node in the displaced Newtonian fluid we have the choice of assigning those nodes associated with the partially filled boundary chambers to be in one phase or the other. When such nodes are assigned to the viscous displaced fluid, we call this choice method 1 [Fig. 2(b)]; otherwise, when they are assigned to the inviscid
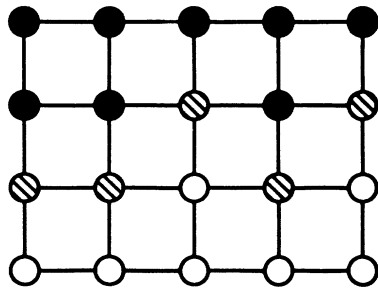
(a)
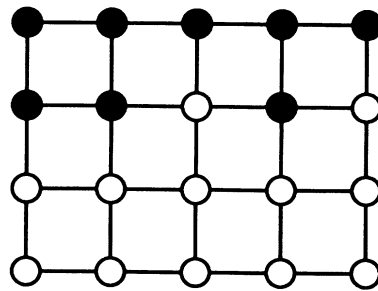
(b)
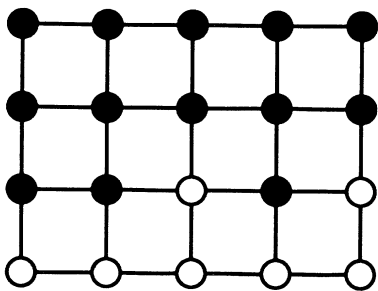
(c)

FIG. 2. The two versions of the tubes and chambers algorithm employed in this paper for the simulation of displacement of a Newtonian viscous fluid by an inviscid fluid, using a two-dimensional square lattice. (a) A typical configuration in the neighborhood of the two-fluid interface for the tubes and chambers model. Black circles denote chambers filled entirely with the inviscid fluid, and white circles denote chambers filled entirely with the Newtonian fluid. The remaining (shaded) circles denote chambers in which both fluids are present. (b) Method 1. With the fluid configuration shown above, for calculations of the pressure field, a boundary chamber is regarded as belonging to the Newtonian fluid. (c) Method 2. With the fluid configuration shown above, for calculations of the pressure field, a boundary chamber is regarded as belonging to the inviscid fluid.

driving fluid, we call the choice method 2 [Fig. 2(c)]. These two choices give different values to the pressure at the boundary nodes and correspond to the two possible ways of implementing the diffusion-limited aggregation algorithm to simulate fluid fingering. The case in which the walker is added to the cluster only if he actually steps on to the cluster (the "Kadanoff method") corresponds to method 1 here. Method 2 is like the standard diffusion-limited aggregation algorithm in which the walker is stuck to the aggregate as soon as he lands onto a site adjacent to the cluster (the "Witten-Sander method"). A more detailed comparison of these and other methods of simulating flow in porous media is given in Sec. IV.

Since time does not appear explicitly in the governing equations, the fluid interface evolves according to the following recipe. For a given fluid interfacial shape, we first identify the set of boundary nodes labeled $\{i\}$ whose chambers are either partially filled by the driving fluid or have the potential of being filled by the driving fluid at the next time step. In method 1, Fig. 2(b), the boundary nodes are in the displaced Newtonian fluid while in method 2, Fig. 2(c), the boundary nodes $\{i\}$ are in the driving inviscid fluid. We now solve the discretized Laplace equation for the pressure distribution P in the driven Newtonian fluid. The interface is then advanced to the next time step by locating, among the set of boundary nodes $\{i\}$, the node which has the minimum value of $(\phi_i / |\nabla P|_i)$—we call this node j. Thus node j is the first boundary node whose chamber will be completely filled by the driving inviscid fluid under the pressure field corresponding to the current fluid interface configuration. We now update the fluid interface by setting node j to be totally within the invading inviscid fluid and all its neighboring nodes whose chambers still contain the original Newtonian fluid will now be identified as part of the new set of boundary nodes. The cycle of solving for the pressure distribution corresponding to this new configuration of the interface is repeated until the interface breaks through at withdrawal point.

At each time step, apart from advancing one transition node, we also *partially fill* each of the remaining chambers in the set $\{i\}$ of transition nodes by the invading inviscid fluid. This corresponds to replacing the fluid capacity of every transition node by

$$\phi_i \rightarrow \phi_i - (\phi_j / |\nabla P|_j) |\nabla P|_i . \tag{3.1}$$

The results of the displacement of a Newtonian fluid by an inviscid fluid are summarized in Table III. Here we display the recovery efficiency—defined as the fraction of chamber volume containing the driving fluid at breakthrough. The results are based on an average of 20 runs using different sets of chamber volumes obeying the same exponential distribution. Of the total amount of fluid driven out of the porous material, about 60% from chambers which have been totally filled by the driving fluid while the remaining 40% or so comes from the boundary chambers which are only partially filled by the driving fluid. In order to make comparison with recovery efficiencies obtained using simulations based on random-walk algorithms we also list the recovery efficiences based

TABLE III. Simulation of recovery efficiency for displacement of a viscous fluid by an inviscid fluid in a quarter five-spot configuration. The simulations (on an $N \times N$ square lattice), are based on the "tubes-and-chambers" model introduced in Sec. II, with an exponential probability density function for the chamber volumes. In method 1 the boundary nodes are in the displaced Newtonian viscous fluid. In method 2 the boundary nodes are in the driving inviscid fluid. The recovery efficiency is calculated by two different definitions: node % is the percentage of nodes from which the viscous fluid is displaced, and volume % is the percentage of the original volume of viscous fluid which is displaced. For each value of N, the recovery efficiency is the average over 20 realizations of the random system. The errors stated are ± 1 standard deviation.

	Method 1		Method 2	
N	Node %	Volume %	Node %	Volume %
10	37.5±6.8	39.7±7.7	27.3±4.1	28.4±5.7
20	29.3±3.5	30.0±4.8	20.2±2.4	19.8±3.2
30	23.9±3.0	24.0±3.0	15.9±2.4	15.9±2.7
40	21.9±2.6	22.0±3.1	14.2±1.5	14.0±1.5
50	21.1±2.8	21.4±2.8	14.1±1.7	14.2±1.5
100	15.9±1.3	16.1±1.2	10.9±1.0	10.9±1.2

on the fraction of nodes that are in the driving inviscid phase at breakthrough. The two estimates of the recovery efficiencies are indistinguishable within statistical fluctuations. This is perhaps unexpected, given the large number of partially-filled chambers at the two-fluid interface when the inviscid fluid reaches the withdrawal point. We have also performed some simulations with the exponential fluid capacity density replaced by a uniform density on the interval (0,1). The results appear in Table IV. With the uniform density of fluid capacities or chamber volumes, the recovery efficiences estimated from percentages of nodes from which viscous fluid is displaced and from percentages of total volume of viscous fluid displaced are no longer close together.

The approximate equivalence of node- and volume-based recovery efficiencies is one of the many remarkable consequences of an exponential fluid capacity density. We collect in Table V the results of simulations of recovery efficiencies based on two diffusion-limited aggregation algorithms. The algorithms used, the Kadanoff algorithm and the Witten-Sander algorithm, are described in more detail in Sec. IV, but we note for the present the equivalence, within statistical fluctuations, of (i) the Ka-

danoff algorithm recovery efficiency and the recovery efficiency of a tubes and chambers simulation by method 1 with exponential fluid capacity density, and (ii) the Witten-Sander recovery efficiency and the recovery efficiency of a tubes and chambers simulation by method 2 with an exponential fluid capacity density. In contrast, comparing Tables IV and V, neither diffusion-limited aggregation algorithm gives recovery efficiencies close to tubes and chambers simulations for uniform fluid capacity density for methods 1 or 2, with either of the two definitions of recovery efficiency.

A detailed comparison between the present physical method of simulating fluid displacement, based on tubes and chambers, and the various heuristic random-walk algorithms is given in Sec. IV.

IV. LATTICE GROWTH MODELS AND FINGERING IN POROUS MEDIA

In Sec. III, we have discussed the practical implementation of our tubes and chambers simulation approach, and reported some representative calculations. We now summarize a number of stochastic simulation algorithms

TABLE IV. Simulation of recovery efficiency for displacement of a viscous fluid by an inviscid fluid in a quarter five-spot configuration, as in Table III, but with the exponential probability density function for the chamber volumes replaced by a uniform density on the unit interval. In method 1 the boundary nodes are in the displaced Newtonian viscous fluid. In method 2 the boundary nodes are in the driving inviscid fluid. The recovery efficiency is calculated by two different definitions: node % is the percentage of nodes from which the viscous fluid is displaced, and volume % is the percentage of the original volume of viscous fluid which is displaced. For each value of N, the recovery efficiency is the average over 20 realizations of the random system. The errors stated are ± 1 standard deviation.

	Method 1		Method 2	
N	Node %	Volume %	Node %	Volume %
10	44.6±5.6	52.2±7.3	30.6±3.9	37.4±5.1
20	35.9±4.7	43.0±5.4	22.6±3.0	28.9±3.8
30	30.7±3.1	36.0±4.1	18.6±1.5	23.7±2.5
40	28.5±2.9	34.2±3.7	16.7±2.1	21.7±2.8
100	19.8±0.6	24.0±0.9	12.5±1.3	16.5±1.6

TABLE V. Simulation of recovery efficiency for displacement of a viscous fluid by an inviscid fluid in a quarter five-spot configuration by diffusion-limited aggregation. In the simulations (on an $N \times N$ square lattice) two DLA algorithms are used. In the "Kadanoff algorithm," the walker is added to the cluster at the site he occupied immediately before stepping onto the cluster. In the "Witten-Sander algorithm" (standard DLA), the walker is added to the cluster immediately he steps onto a site adjacent to the cluster. The recovery efficiency is calculated from the percentage of nodes (lattice sites) from which the viscous fluid is displaced. For each value of N, 20 runs were made. The efficiency displayed is the mean and the errors stated are ±1 standard deviation.

N	Kadanoff algorithm	Witten-Sander algorithm
10	38.7±6.9	29.2±3.9
20	28.4±3.8	20.3±3.0
30	26.7±3.9	16.9±2.4
40	22.7±2.8	15.2±1.8
50	20.2±1.8	14.1±1.5
100	16.1±1.5	11.2±1.1

which have been used to describe fingering in porous media and compare them with our present simulation method. We are specifically interested in flow in porous media here and we shall not discuss stochastic algorithms that have been designed to model Hele-Shaw cells rather than porous media.

A. Phenomenological algorithms

1. The Witten-Sander algorithm (classical diffusion-limited aggregation or DLA).

In the algorithm proposed by Witten and Sander[8] for the simulation of aggregation processes, random walkers are released one at a time from a source point or source line, and diffuse until they reach a site adjacent to the cluster, where they stick. Paterson[9] noted the identity between the continuum limit of the diffusion-limited aggregation process and the Darcy equations for describing simultaneous flow of a Newtonian fluid and an inviscid fluid through a porous medium. This suggests the possibility of simulating stable and unstable displacements in porous media and Hele-Shaw cells using diffusion-limited aggregation. Paterson's simulations, based on the diffusion-limited-aggregation algorithm, reproduced displacement patterns that are very similar to fingering in porous media, but much less like Hele-Shaw cell flow patterns. The qualitative explanation is that in Hele-Shaw cells fluctuations in the physical parameters that control flow are very small compared to those in porous media.

2. The Kadanoff algorithm

This algorithm[19] is very similar to the Witten-Sander algorithm. The walkers are released one at a time, and move at random until they step onto an occupied site, at which time another random walker is released. Walkers are added to the cluster at the sites they occupied immediately prior to stepping onto the cluster. Other as-

pects of Kadanoff's algorithm and its generalizations,[20] concerned with the problem of incorporating surface tension effects into Hele-Shaw cell problems, are inappropriate for porous media, and we shall not discuss them here.

3. The Niemeyer-Pietronero-Weismann algorithm (dielectric breakdown model).

As a model of dielectric breakdown, Niemeyer et al.[21] proposed the following algorithm governing stochastic interface growth. A discrete version of Laplace's equation is solved subject to a prescribed constant value of the unknown function at the boundary. In the context of the two-phase flow problem, the unknown function is the pressure, so the simulation is appropriate only to the case of a viscous fluid and an inviscid fluid. For the unstable case, inviscid displacing viscous, it is customary to speak of the displacement as occurring at infinite mobility ratio. At each step one site on the boundary is selected at random for growth, the probability of selection being proportional to the gradient of the unknown function, i.e., to the pressure gradient or volume flux. The algorithm of Niemeyer et al. is sometimes called the dielectric breakdown model (DBM). It should be noted that the same acronym is used by Ben Jacob et al.,[22] to denote dense branching morphology, which is their view of the experimental outcome of a fingering experiment.

4. Gradient-governed growth

As a specific model of flow in porous media, Sherwood and Nittmann[23] introduced an algorithm they called gradient-governed growth. The name diffusion-limited growth (DLG), is sometimes also used for this algorithm. This algorithm is the extension of the Niemeyer-Pietronero-Weismann algorithm to the case of two viscous fluids, rather than an inviscid fluid displacing a viscous one, i.e., to the case of finite mobility ratio. A discrete version of Laplace's equation is solved in the regions occupied by each fluid to yield the pressure, which is constrained to be continuous at each point on the two-fluid interface. One point on the interface is advanced at each time step, with the selection probabilities proportional to the local pressure gradient. As the viscosity of the injected fluid increases, i.e., as the mobility ratio is reduced, in the algorithm of Sherwood and Nittmann the fingers become thicker and grow more slowly in length.

5. Algorithms with tunable noise

The Hele-Shaw cell corresponds, in a sense, to a porous medium with no microstructure induced noise, though of course one needs some source of noise in the system to set off the instability. The Witten-Sander and Niemeyer-Pietronero-Weismann algorithms described above are found to be too noisy, and for qualitatively correct simulation of flow in Hele-Shaw cells, it is essential to reduce the noise of the diffusion-limited-aggregation algorithm. Methods of reducing the noise have been discussed by Daccord et al.[17] and by Liang.[24] Typically, the noise of the algorithm is reduced by insisting that random walkers must strike a site several times before the interface ad-

vances. Liang also models the effect of surface tension in a Hele-Shaw cell by allowing walkers to originate not only at the pressure sources or sinks but also at the two-fluid interface itself; this treatment of surface tension is not applicable to chaotic porous media.

As we noted at the end of Sec. III from our simulation results for the quarter five-spot configuration (Tables III and V) with an exponential fluid capacity density, the recovery efficiencies for Kadanoff's algorithm are statistically equivalent to a tubes and chambers simulation by method 1, and the recovery efficiencies for the Witten-Sander algorithm are statistically equivalent to a tubes and chambers simulation by method 2. The equivalence of a phenomenological rule (DLA, with no medium microstructure, only one point on the interface evolving at a time, and an efficiency based on the percentage of sites displaced) and a physically based algorithm (the tubes and chambers model, with medium microstructure, all points on the interface evolving with time simultaneously, and an efficiency based on percentages of volume displaced) merits explanation.[25] The explanation must highlight the special significance of an exponential fluid capacity density, since it is for this special microstructure, rather than for arbitrary microstructure, that the two fundamentally different approaches yield statistically equivalent results. For the differences between an exponential fluid capacity density and a uniform density in two-dimensional simulations, one need only compare Tables III and IV. One-dimensional tubes and chambers simulations have been reported previously.[7] Of the variety of densities chosen in the earlier paper, only the exponential distribution gave recovery efficiences close to those for a diffusion-limited-aggregation simulation.

B. Connecting random walks with physics

We shall now establish a quantitative connection between fingering in random porous media (where the length scales involved with the fingering are heavily coupled to the microstructure), and stochastic algorithms phrased in terms of uniform media (where all randomness enters from the tortuous trajectories of random walkers or from phenomenological rules coupling advance probabilities to the shapes of boundaries). To develop the connection, we first consider two purely phenomenological rules, one of which is divorced from microstructure, while the other is coupled to microstructure, but not yet tied to hydrodynamics. We develop precise conditions under which the conceptually distinct rules are mathematically identical. The microstructure-based rule is then shown to coincide approximately with the tubes and chambers simulation algorithm. The analysis brings out the special significance of exponentially distributed fluid capacity.

1. A relation between two phenomenological rules.

The setting for both the phenomenological rules is the same. We consider any connected set of sites on a d-dimensional lattice, with a single new site about to be added to the cluster in a random fashion. We label the possible bonds along which the growth may occur, i.e.,

all bonds adjacent to the cluster, with an index $i = 1, 2, \ldots, N$. With each of these bonds is associated a deterministic positive number v_i (called for convenience a "flux") and a positive random variable ϕ_i. For the fluid displacement problem under consideration v_i denotes the volume flux calculated on the basis of Darcy's law (1.2), ϕ_i is a fluid capacity associated with site i and v_i/ϕ_i is the instantaneous velocity of the appropriate interface. We consider two prescriptions for the probability that the bond labeled i is the bond chosen for growth: the "flux rule"

$$\mathrm{Pr}\{\text{bond } i \text{ chosen}\} = \frac{v_i}{\sum\limits_{j=1}^{N} v_j} \; , \tag{4.1}$$

and the "speed rule"

$$\mathrm{Pr}\{\text{bond } i \text{ chosen}\} = \mathrm{Pr}\{v_i/\phi_i = \max[v_j/\phi_j]\} \; , \tag{4.2}$$

respectively. In the degenerate case in which all of the fluxes v_i are equal, the speed rule becomes

$$\mathrm{Pr}\{\text{bond } i \text{ chosen}\} = \mathrm{Pr}\{\phi_i = \min[\phi_j]\} \; . \tag{4.3}$$

Equation (4.3) is the defining equation of the invasion percolation model of Lenormand and Bories and Chandler *et al.*[26]. In the context of the fluid displacement problem, the speed rule is thus a generalization of the invasion percolation model.[27]

In an earlier paper,[7] the flux rule and the speed rule were called hypothesis A and hypothesis B, respectively; the present names convey the essence of the algorithms. The flux rule is the basis of the Niemeyer-Pietronero-Weismann algorithms, and has been in use for some time.[24,28,29] When the fluxes are derived as the gradients of solutions of Laplace's equation, the flux rule is well known to be equivalent to diffusion-limited aggregation. The speed rule was proposed by the authors only recently.[7] Let f denote the probability density function for the independent random variables ϕ_i. The event "$v_i/\phi_i = \max(v_j/\phi_j)$" is exactly the same as the event "$\phi_j \geq (v_j/v_i)\phi_i$ for all j," so that Eq. (4.2) becomes

$$\mathrm{Pr}\{\text{bond } i \text{ chosen}\}$$

$$= \int_0^\infty d\phi_i f(\phi_i) \prod_{\substack{j=1 \\ j\neq i}}^{N} \int_{(v_j/v_i)\phi_i}^{\infty} d\phi_j f(\phi_j) \; . \tag{4.4}$$

For the special case in which the random variables ϕ_i have the exponential density $f(\phi) = \alpha \exp(-\alpha\phi)$, where α is an arbitrary constant, the integrals in Eq. (4.4) are easily evaluated and the probability found to be $v_i/\sum_j v_j$. Hence the two growth laws (4.1) and (4.2) are exactly the same, irrespective of the precise values of the deterministic quantities v_i and the value of N, provided that the random variables ϕ_i are exponentially distributed. This result may be significant for the modeling of a variety of processes in which there is both a deterministic field and a random transport coefficient governing interface motion. For the particular problem of fluid displacements in porous media it will enable us to construct a direct connection between diffusion-limited aggregation

and fingering in a tubes and chambers model of a porous medium with exponentially distributed fluid capacity.

2. The essence of a tubes and chambers simulation

In a tubes and chambers simulation, fluid is allowed to flow at all positions on the interface, so that the process takes place in continuous time and something is happening at all interface sites. This is in apparent contrast with the flux and speed rules above, in which only one site evolves at each discrete time step. However, we can convert the tubes and chambers algorithm into a discrete time process, as follows. Let the chambers at the interface sites have unfilled volumes ϕ_i^* and fluxes v_i feeding them. (The asterisk is to remind us that the random volumes remaining to be filled to not in general have the same statistical distribution as the virgin volumes ϕ_i.) Nothing happens to the position of the interface until one of the partially filled chambers is filled. The time to fill chamber i is simply ϕ_i^*/v_i, so that to convert the tubes and chambers simulation to a discrete-time process, we need only locate the chamber which fills first, by finding the minimum of ϕ_j^*/v_j as the index j runs over the boundary sites. Let us assume that the ith chamber is the quickest to fill. We now fill this chamber instantaneously and advance the interface to a new virgin chamber, while reducing the volumes of all other chambers at the interface appropriately: ϕ_j^* is replaced by $\phi_j^* - v_j \phi_i^*/v_i$. Although this observation enables us to reduce the simulation to a discrete-time process, it is in general, at the cost of pushing the statistical distribution of the volumes to be filled further and further from the distribution governing virgin chambers.[30] While this complication applies at all sites, it is well established by simulation and experiment that the growth process in fingering (and similar processes) is almost exclusively confined to tip regions. In appropriate geometries, the fluxes near the growing tips may exhibit radial or other symmetries, so that all points at which interface advance is reasonably likely to occur experience approximately equal fluxes ($v_j/v_i \approx 1$). The growth step thus consists of selecting the smallest value ϕ_i^* of the unfilled chamber volumes at the preferred growth sites, filling the associated chamber, and reducing the volumes of all other chambers at the interface by ϕ_i^*.

3. Restoration of innocence

The exponential density has a remarkable property which one may describe colloquially as "restoration of innocence." Let us consider two independently and identically distributed random variables ϕ_1 and ϕ_2, with a common probability density function f. The variables ϕ_1 and ϕ_2 may be envisaged as the volumes of two virgin chambers. Let us being filling each of the two chambers with fluid entering at the same rate. In general, the two chambers will not have equal volumes, and $|\phi_1 - \phi_2|$ will be the volume remaining to be filled in the larger chamber when the smaller chamber has just been filled. The quantity $\phi = |\phi_1 - \phi_2|$ is itself a random variable, and it is straightforward to show that its probability density function is

$$g(\phi) = 2\int_0^\infty f(\xi + \phi)f(\xi)d\xi . \qquad (4.5)$$

In general, $f(\phi) \neq g(\phi)$, so that the random volumes of virgin chambers and partially filled chambers have different distributions. For example, if $f(\phi)=1$, $0<\phi<1$ [and $f(\phi)=0$ otherwise] we find that $g(\phi)=2(1-\phi)$, $0<\phi<1$ [and $g(\phi)=0$ otherwise]. However, in the special case in which ϕ_1 and ϕ_2 have the exponential density $f(\phi)=\alpha \exp(-\alpha\phi)$, we find that $g(\phi)=\alpha \exp(-\alpha\phi)$, so that the random unfilled volume $\phi = |\phi_1 - \phi_2|$ is indistinguishable from a new random chamber. With exponentially distributed chambers and a constant value of the flux v_j at the preferred growth sites, the tubes and chambers model corresponds to a simulation based on the speed rule with "fluxes" v_j. The only error in this identification is associated with sites not close to the growing tips, which are of small statistical significance.

It may be remarked in passing that we have not used any property of the v_j beyond approximate consistency at the growing sites, so that the argument should apply to non-Newtonian flow problems as easily as to Newtonian ones. The simulations reported in Sec. III are for incompressible Newtonian fluids, and the volumes fluxes in the tubes are determined by the solution of the discrete Laplace equation. To extend them to non-Newtonian fluids requires the specification of a flow law nonlinear in the pressure gradient for each tube, so that the discrete Laplace equation is replaced with a nonlinear system of equations. The present tubes and chambers algorithm is thus as applicable to non-Newtonian fluids as the algorithms based on the dielectric breakdown model. For Newtonian fluids, the tubes and chambers approach is not especially cheap to run; neither are the dielectric-breakdown model algorithms or other simulation schemes[31] proposed for porous media or the Hele-Shaw cell. Algorithms based on diffusion-limited aggregation are much cheaper to run, but are not applicable to all microstructure distributions. For instance, for the tubes and chambers simulation of two-fluid displacement, the diffusion-limited-aggregation alternative is available only for an exponential fluid capacity distribution. Since we are at liberty to vary the length scale in simulations, it is in principle possible to select a length scale on which a random-walk-based simulation is least in error, by adjusting the length scale to obtain to fluid capacity distribution as close to possible to exponential. In this context, the natural emergence of the exponential distribution as the distribution of greatest entropy at fixed mean fluid capacity is most satisfying.

In attempting to explain the statistical equivalence between diffusion-limited-aggregation and two-fluid displacement processes in structurally random porous media, we have used a number of intermediate phenomenological models, including the essentially new speed rule [Eq. (4.2)] and the previously proposed flux rule [Eq. (4.1)]. It is possible to decorate these phenomenological models in many ways, but such an exercise is more one of mathematics than one of physics, and detracts attention from the key issue. The key issue addressed in the present paper has been the development of practical,

physically-based simulation schemes for two-phase porous medium flow, in which structural information is quantitatively included. The concept of fluid capacity and its incorporation into the tubes and chambers algorithm captures the essential physics of two fluid displacement processes in random porous media. The use of the diffusion-limited-aggregation method to visualize flow patterns is appropriate only under very special conditions as outlined above.

[1]If the dynamical effects of interfacial tensions between the two fluids and between fluid and solid are to be included, a pressure difference exists between the phases. This pressure difference, a function of the relative saturations of the two phases in a small but finite region, is called the capillary pressure. Capillarity also ensures that the two phases sample different regions of the pore space, and the permeability k in Darcy's law has to be replaced by saturation and history-dependent relative permeabilities. See, for example, C. M. Marle, *Multiphase Flow in Porous Media* (Gulf, New York, 1981). Our neglect of capillary effects is most appropriate to the case of the displacement of one viscous fluid by a fluid of very much smaller viscosity (for example, displacing water by air) so that pressure gradients in the less viscous fluid may be neglected.

[2]J. H. S. Hele-Shaw, Nature **58**, 34 (1898); Trans. Inst. Naval Architects London **40**, 21 (1898).

[3]There are many papers in the literature on this subject, beginning with the classic paper of P. G. Saffman and G. I. Taylor, Proc. R. Soc. London, Ser. A **245**, 312 (1958); a recent paper is D. Bensimon, Phys. Rev. A **33**, 1302 (1986). The original Saffman-Taylor paper considered only linear fingers. For radial fingering, see L. Paterson, J. Fluid Mech. **113**, 513 (1981).

[4]See the experiments on transparent consolidated porous media by L. Paterson, Powder Technol. **36**, 71 (1983), and those on etched networks by R. Lenormand and C. Zarcone, J. Fluid Mech. **135**, 337 (1983); Phys. Rev. Lett. **54**, 2226 (1985); J.-D. Chen and D. Wilkinson, Phys. Rev. Lett. **55**, 1892 (1985).

[5]J. Bear, *Dynamics of Fluids in Porous Media* (Elsevier, New York, 1972).

[6]J. Bear and Y. Bachmat, in *Fundamentals of Transport in Porous Media*, Vol. E82 of *NATO Advanced Study Institute Series*, edited by J. Bear and M. Y. Corapcioglu (Nijhoff, Boston, 1982).

[7]D. Y. C. Chan, B. D. Hughes, and L. Paterson, Phys. Rev. A **34**, 4079 (1986).

[8]T. A. Witten and L. M. Sander, Phys. Rev. Lett. **47**, 1400 (1981); and Phys. Rev. B **27**, 5686 (1983). For a recent review of DLA and related models see P. Meakin, in *On Growth and Form*, edited by H. E. Stanley and N. Ostrowsky (Nijhoff, Boston, 1986), pp. 111–135.

[9]L. Paterson, Phys. Rev. Lett. **52**, 1621 (1984).

[10]D. Y. C. Chan, B. D. Hughes, and L. Paterson, Transport in Porous Media **3**, 81 (1988).

[11]W. Feller, *An Introduction to Probability Theory and Its Applications*, 2nd ed. (Wiley, New York, 1971), Vol. 2.

[12]This problem is related to many problems of percolation and conduction in random media. Permeabilities for network models of porous media have been analyzed by J. Koplik, J.

Fluid Mech. **119**, 219 (1982); J. Phys. C **14**, 4821 (1981).

[13]C. Shannon, Bell Syst. Tech. J. **27**, 379 (1948); **27**, 623 (1948).

[14]S. A. Trugman, Phys. Rev. Lett. **57**, 607 (1986).

[15]G. Daccord, J. Nittmann, and H. E. Stanley, in *On Growth and Form*, edited by H. E. Stanley and N. Ostrowsky (Nijhoff, Boston, 1986), pp. 203–210; Phys. Rev. Lett. **56**, 336 (1986); J. Nittmann, G. Daccord, and H. E. Stanley, in *Fractals in Physics*, edited by L. Pietronero and E. Tossati (Elsevier, Amsterdam, 1986), pp. 193–202.

[16]D. Y. C. Chan, B. D. Hughes, and L. Paterson, Nature **325**, 489 (1987).

[17]See, e.g., Ref. 8.

[18]L. Colgan, in *Computational Techniques for Differential Equations*, edited by J. Noye (Elsevier, Amsterdam, 1984).

[19]L. P. Kadanoff, J. Stat. Phys. **39**, 267 (1985).

[20]E.g., C. Tang, Phys. Rev. A **31**, 1977 (1985); S. Liang, *ibid.* **33**, 2663 (1986); M. Sahimi and Y. Yortsos, *ibid.* **32**, 3762 (1985).

[21]L. Niemeyer, L. Pietronero, and H. J. Weismann, Phys. Rev. Lett. **52**, 1033 (1984).

[22]E. Ben-Jacob, Y. Godbey, N. D. Goldenfeld, J. Koplik, H. Levine, T. Mueller, and L. M. Sander, Phys. Rev. Lett. **55**, 1315 (1985).

[23]J. D. Sherwood and J. Nittmann, J. Phys. (Paris) **47**, 15 (1986).

[24]S. Liang, Ref. 20.

[25]That there is a "natural correspondence" between method 1 and Kadanoff's algorithm can be seen as follows. In Kadanoff's algorithm there is nonzero probability that a walker will step onto a site adjacent to the cluster without sticking. Remembering that pressure in the viscous fluid corresponds to a random-walk probability, the sites at which growth may occur, viz., the boundary chambers, must be at a pressure different to that in the inviscid fluid. The boundary chambers are therefore identified for pressure calculations as belonging to the Newtonian viscous fluid. A similar "natural correspondence" between method 2 and the Witten-Sander algorithm is easily argued. However, seeing a natural correspondence is far short of establishing a quantitative connection.

[26]R. Lenormand and S. Bories, C. R. Acad. Sci. Paris B **291**, 279 (1980); R. Chandler, J. Koplik, K. Lerman, and J. F. Willemsen, J. Fluid Mech. **119**, 249 (1982); B. Nickel and D. Wilkinson, Phys. Rev. Lett. **51**, 71 (1983); D. Wilkinson and J. F. Willemsen, J. Phys. A **16**, 3365 (1983); J. T. Chayes, L. Chayes, and C. M. Newman, Commun. Math. Phys. **101**, 383 (1985).

[27]Another connection between invasion percolation and a stochastic growth process on a uniform lattice has been made by H. Mártin, J. Vannimenus, and J. P. Nadal, Phys. Rev. A **30**, 3205 (1984). Mártin *et al.* phrase their model in terms of a

cell-growth process, placing random variables analogous to energies at each site, which determine the probabilities of growth at that site according to a Boltzmann-type distribution. The Eden model [M. Eden, *Proceedings of the 4th Berkeley Symposium on Mathematical Statistics and Probability,* edited by J. Neyman (University of California Press, Berkeley, California, 1961), Vol. 4, p. 223; D. Richardson, Proc. Cambridge Philos. Soc. **74**, 515 (1973)] is recovered in the limit of zero "temperature." There is no analogue in their system of the flux v_j introduced in our discussion. The crossover between the Eden model and invasion percolation is also examined in detail by J. P. Nadal, R. M. Bradley, and P. N. Strenski, J. Phys. A **19**, L505 (1986), using a class of one-dimensional models related to the model of Mártin *et al.*, but again there is no analogue of the flux v_j.

[28] A. J. DeGregoria, Phys. Fluids **38**, 2933 (1985).

[29] M. J. King and H. Scher, Phys. Rev. A **35**, 929 (1987).

[30] The following observation is of some interest, but we present it as clearly identified digression from the main discussion to prevent it from obscuring the flow of the argument. The change in the effective fluid capacity distribution is a nuisance. As a purely phenomenological model, with no physical basis claimed, one might maintain the original distribution of fluid capacities by advancing only one boundary node per time step, but instead of partially filling the remaining boundary nodes, reassigning new fluid capacities to these nodes according to the specified fluid capacity distribution. With this modification of the simulation algorithm, all subsequent advances of the fluid interface are based on a selection process in which all the boundary chambers have identical and independent distribution of fluid capacities. We have observed from our calculations that the displacement efficiencies obtained with partial filling option (the original tubes and chambers scheme) or the fluid capacity reassignment option (proposed in this digression) are identical within statistical fluctuations, for the exponential distribution.

[31] Boundary integral methods have been used by A. J. DeGregoria and L. W. Schwartz, Phys. Fluids **28**, 2313 (1986). A vortex sheet simulation has been employed by G. Tryggvason and H. Aref, J. Fluid Mech. **136**, 1 (1983).